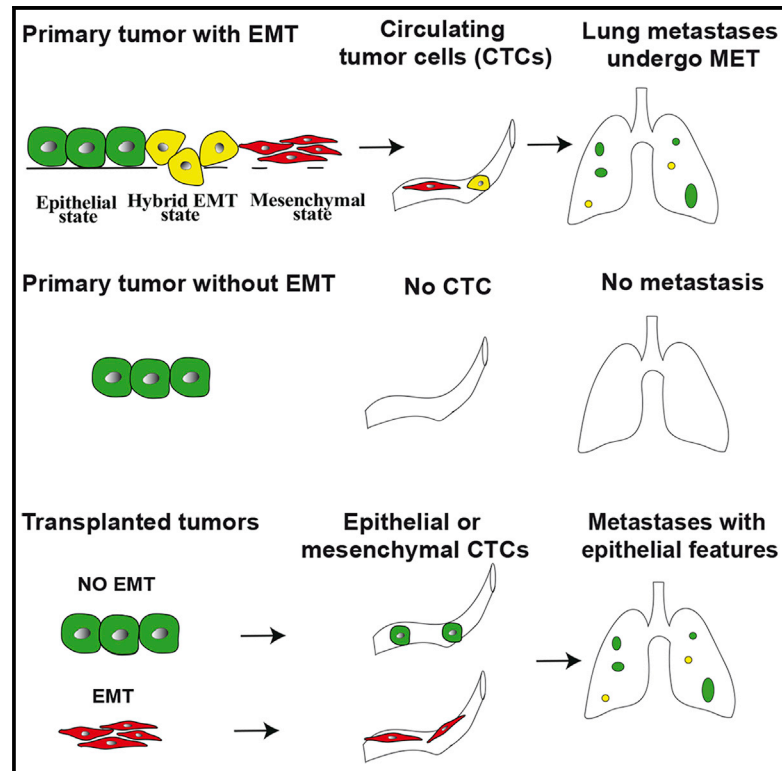


## Context Dependency of Epithelial-to-Mesenchymal Transition for Metastasis

### Graphical Abstract



### Highlights

- Primary skin SCCs with EMT have a high incidence of metastasis
- Primary skin SCCs without EMT have no metastasis
- Circulating tumor cells present EMT in primary tumors with metastasis
- Transplanted tumors present metastasis regardless of EMT

### Authors

Tatiana Revenco, Adeline Nicodème, Ievgenia Pastushenko, ..., Sophie Lemaire, Viviane de Maertelaer, Cédric Blanpain

### Correspondence

cedric.blanpain@ulb.ac.be

### In Brief

The role of epithelial-to-mesenchymal transition (EMT) during metastasis remains controversial. Revenco et al. show that in models of primary skin tumors, only EMT tumors are associated with metastasis. In contrast, EMT is not required to induce metastasis following the subcutaneous transplantation of tumor cells, demonstrating the context dependency of EMT for metastasis.



# Context Dependency of Epithelial-to-Mesenchymal Transition for Metastasis

Tatiana Revenco,<sup>1</sup> Adeline Nicodème,<sup>1</sup> Ievgenia Pastushenko,<sup>1</sup> Magdalena K. Sznurkowska,<sup>1</sup> Mathilde Latil,<sup>1</sup> Panagiota A. Sotiropoulou,<sup>1</sup> Christine Dubois,<sup>1</sup> Virginie Moers,<sup>1</sup> Sophie Lemaire,<sup>1</sup> Viviane de Maertelaer,<sup>2</sup> and Cédric Blanpain<sup>1,3,4,\*</sup>

<sup>1</sup>Laboratory of Stem Cells and Cancer, Université Libre de Bruxelles, Brussels 1070, Belgium

<sup>2</sup>IRIBHM, Université Libre de Bruxelles, Brussels 1070, Belgium

<sup>3</sup>WELBIO, Université Libre de Bruxelles, Brussels 1070, Belgium

<sup>4</sup>Lead Contact

\*Correspondence: [cedric.blanpain@ulb.ac.be](mailto:cedric.blanpain@ulb.ac.be)

<https://doi.org/10.1016/j.celrep.2019.09.081>

## SUMMARY

Epithelial-to-mesenchymal transition (EMT) has been proposed to be important for metastatic dissemination. However, recent studies have challenged the requirement of EMT for metastasis. Here, we assessed in different models of primary skin squamous cell carcinomas (SCCs) whether EMT is associated with metastasis. The incidence of metastasis was much higher in SCCs presenting EMT compared to SCCs without EMT, supporting the notion that a certain degree of EMT is required to initiate the metastatic cascade in primary skin SCCs. Most circulating tumor cells presented EMT, whereas most lung metastasis did not present EMT, showing that mesenchymal-to-epithelial transition is important for metastatic colonization. In contrast, immunodeficient mice transplanted with SCCs, whether displaying EMT or not, presented metastasis. Altogether, our data demonstrate that the association of EMT and metastasis is model dependent, and metastasis of primary skin SCCs is associated with EMT.

## INTRODUCTION

Cancer metastasis, which represents the propagation of primary tumor cells in distant tissues, is the leading cause of cancer patient mortality (Mehlen and Puisieux, 2006; Mittal, 2018). Metastasis involves a series of distinct biological processes known as the metastatic cascade (Lambert et al., 2017; Massagué and Obenauf, 2016). Tumor cells (TCs) need to invade the microenvironment of the primary tumor, intravasate and circulate into the blood or lymphatic circulation, reach distant organs, extravasate from the circulation into the metastatic site, colonize this organ, and proliferate and establish the secondary tumor(s). While the mutations and molecular mechanisms necessary to initiate tumor formation are relatively well characterized, the precise molecular events responsible for the different steps of the metastatic cascade are much less un-

derstood (Diepenbruck and Christofori, 2016; Nieto et al., 2016).

It has been proposed that epithelial-to-mesenchymal transition (EMT)—a developmental process that allows epithelial cells to detach from their neighboring cells, lose some of their epithelial characteristics, and acquire mesenchymal features, such as their ability to migrate as individual cells—is important to initiate the metastatic cascade allowing the cancer cells to leave the primary tumor, invade, and migrate across the surrounding mesenchyme to reach the circulation (Massagué and Obenauf, 2016; Nieto et al., 2016). Since most of the metastases present a low degree of EMT, it has been suggested that EMT TCs undergo mesenchymal-to-epithelial transition (MET) at the metastatic site (Chaffer et al., 2007; Gunasinghe et al., 2012; Nieto et al., 2016; Yao et al., 2011).

Short hairpin RNA (shRNA) or small interference RNA (siRNA) knockdown of transcription factors (TFs) that promote the EMT, such as Twist1, Snai1, or Prrx1, in different cancer cell lines transplanted into immunodeficient mice decreases metastasis in these experimental conditions (Olmeda et al., 2007; Takano et al., 2016; Tsai et al., 2012; Xu et al., 2017; Yang et al., 2004). The conditional deletion of Zeb1, a key EMT TF in a mouse model of a pancreatic tumor, strongly decreases the proportion of mice with metastasis (Krebs et al., 2017). Conversely, transient overexpression of Twist1 or Prrx1 promotes the circulation of cancer cells into the blood and the formation of distant metastases (Ocaña et al., 2012; Schmidt et al., 2015; Tsai et al., 2012; Yang et al., 2004). However, sustained overexpression of these TFs inhibits metastasis, suggesting that a downregulation of the EMT program is important for the establishment and growth of metastasis (Celià-Terrassa et al., 2012; Ocaña et al., 2012; Stankic et al., 2013; Tsai et al., 2012). An intravenous injection of TCs that undergo EMT, in particular cells that undergo partial EMT, promotes lung colonization and metastasis of mouse skin, pancreatic, and breast tumors (Del Pozo Martin et al., 2015; Latil et al., 2017; Pastushenko et al., 2018; Rhim et al., 2012). Collectively, these data support the importance of EMT in promoting tumor dissemination and metastasis. However, it has been recently shown that the conditional deletion of Snai1 or Twist1 in mouse pancreatic tumors or the overexpression of mir200 in a mouse model of mammary tumors did



not affect the occurrence of metastasis, questioning the importance of EMT for metastasis (Fischer et al., 2015; Zheng et al., 2015).

Many of the aforementioned studies used non-physiological experimental approaches such as intravenous injection of TCs or overexpression of EMT TFs, or they can be associated with other confounding factors, raising the question of whether a spontaneously occurring EMT is required to initiate the metastatic cascade in the most common primary epithelial cancers and whether MET is required to promote metastatic colonization and outgrowth.

The detection of circulating TCs (CTCs) has been shown to be associated with metastatic burden and correlates with poor prognosis in human cancers (Krebs et al., 2014; Pantel et al., 2008). However, the gold standard method to detect CTCs uses Epcam expression, an epithelial marker that is lost during EMT, to monitor the presence of CTCs in the blood of cancer patients or mice with tumors (Krebs et al., 2014). It has recently been shown that some CTCs can lose their epithelial characteristic, including the expression of Epcam or E-cadherin and present mesenchymal features (Yu et al., 2013), suggesting that the expression of Epcam by CTCs can underestimate the number of CTCs. Because it is not possible to unambiguously detect CTCs without fluorescently marked TCs, the exact proportion of EMT CTCs arising from the primary tumors that spontaneously metastasize is currently unknown.

We have recently demonstrated that a physiological level of oncogenic KRas<sup>G12D</sup> expression together with p53 deletion in two distinct compartments of the skin epidermis leads to completely different tumor phenotypes. KRas<sup>G12D</sup>/p53<sup>CKO</sup> in the skin interfollicular epidermis (IFE) using K14CREER leads to the formation of well-differentiated squamous cell carcinoma (SCCs) with no sign of EMT, whereas the same oncogenic hits in hair follicle (HF) lineages using Lgr5CREER lead to tumors presenting EMT (Latil et al., 2017; Pastushenko et al., 2018). The presence and importance of EMT in these tumors can be easily monitored using fluorescence-activated cell sorting (FACS) to quantify the proportion of TCs expressing Epcam (Latil et al., 2017; Pastushenko et al., 2018).

Here, we used these two models of skin SCC in which TCs are fluorescently labeled, and present or do not present a spontaneous EMT, to assess whether the development of spontaneous lung and lymph node metastases in primary cancer mouse models is correlated with EMT without the need for overexpression of EMT TFs or an intravenous injection of TCs. We also used these models to assess whether CTCs undergo EMT and whether MET frequently occurs at the distant metastatic site. Finally, we assessed the association of EMT and metastasis in a frequently used experimental model based on a subcutaneous injection of TCs into immunodeficient mice. Our data indicate that EMT in primary tumors is always associated with the initiation of the metastatic cascade in primary mouse skin SCCs and that MET occurs at the metastatic site. In contrast, EMT is not required to induce metastasis after subcutaneous transplantation of TCs.

## RESULTS

### HF-Derived SCCs with a Spontaneous EMT Present a High Incidence of Metastasis

To determine whether primary skin SCCs presenting EMT are associated with spontaneous metastasis, we assessed metastatic incidence and quantified the degree of EMT in primary skin tumors arising from the expression of KRas<sup>G12D</sup> and p53 deletion in HF lineages using Lgr5CreER/ KRas<sup>G12D</sup>/p53<sup>CKO</sup> /RosaYFP (yellow fluorescent protein) mice (Figure 1A). The presence of Rosa-YFP allowed YFP labeling of the tumor-initiating cells, which enabled the tracking of TCs in primary tumors, CTCs in the blood, and metastasis in distant organs (Latil et al., 2017; Pastushenko et al., 2018). In Lgr5CreER/ KRas<sup>G12D</sup>/p53<sup>CKO</sup> /RosaYFP HF-derived tumors, most SCCs contain EMT TCs (YFP+ Epcam-), although the proportion of EMT TCs varies between the different tumors, ranging from well-differentiated SCCs with only a few percent of Epcam-TCs to fully mesenchymal tumors with more than 90% of Epcam- TCs (Latil et al., 2017) (Figures 1B and S1A).

Lgr5 is expressed in different tissues and organs, including the lung mesenchyme (Lee et al., 2017; Zepp et al., 2017). To avoid oncogene and YFP expression in these different organs, and to induce oncogene expression specifically in the skin epidermis, we applied a low dose of hydroxytamoxifen topically on the backskin of the mice. Using this procedure, we induced YFP expression only in the skin epidermis and not in distant organs such as the lung (Figures 1C–1E). The number of skin tumors varied from mouse to mouse and led to, on average, 3 YFP+ tumors per mouse (Figure S1B).

By analyzing lungs and lymph nodes (LNs) of Lgr5CreER/ KRas<sup>G12D</sup>/p53<sup>CKO</sup>/RosaYFP mice presenting SCCs, we found that 28.6% (20/70) of mice presented lung YFP+ metastases, and 48.6% (34/70) of mice presented LN YFP+ metastases. Almost all mice presenting lung metastases had LN metastases (18/20), and only 2 mice developed exclusively lung metastases (Figures 1F–1H). The timing between the appearance of the primary tumors and the termination of the experiments was similar between mice presenting and not presenting metastasis (Figures S1C and S1D), suggesting that the timing between the tumor occurrence and the development of metastasis was not a confounding variable in this study.

To determine whether the occurrence of metastasis is associated with EMT, we quantified the percentage of YFP+ Epcam-TCs in primary tumors by FACS in mice that developed or did not develop metastasis. In all mice that developed lung or LN YFP+ metastasis, at least one of the SCCs presented some degree of EMT, as shown by the presence of YFP+ Epcam- TCs in these mice (>7.5% YFP+ Epcam- TCs) (Figures 1I and S1E–S1G). In contrast, none of the mice presenting SCCs with a low degree of EMT (<7.5% of YFP+ Epcam- TCs) developed LN or lung metastases (n = 8 mice) (Figure 1J; mice 1–8). The mean percentage of Epcam- TCs for metastatic mice was clearly higher in comparison to non-metastatic mice. When considering the lowest percentage of Epcam values (the most mesenchymal tumors) found among different tumors in a given mouse, the mean percentage of YFP+ Epcam- TCs in tumors of non-metastatic mice was lower than the mean percentage of YFP+

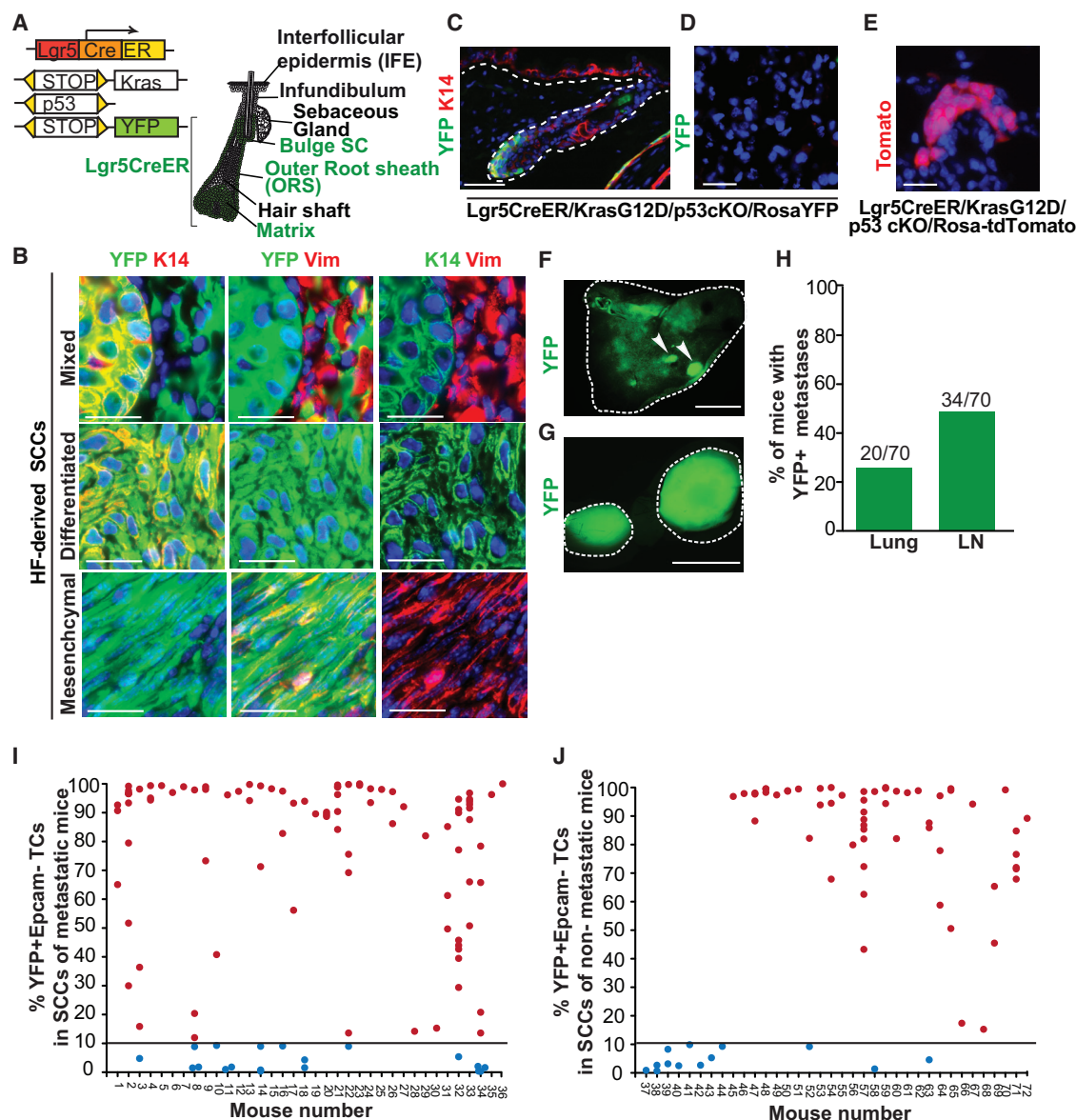


**Figure 1. HF-Derived SCCs with a Spontaneous EMT Present a High Incidence of Metastasis**

(A) Schematic of skin epidermis with its different lineages, and the mouse model of skin SCCs with a high incidence of the EMT induced by *Kras*<sup>G12D</sup> expression and p53 deletion in HF lineage using *Lgr5CreER*.

(B) Immunofluorescent images of mixed SCCs (upper panel), differentiated SCCs (middle panel), and mesenchymal SCCs (lower panel) in *Lgr5CreER/Kras*<sup>G12D</sup>/*p53*<sup>ckO</sup>/*RosaYFP* mice. Scale bars, 50  $\mu$ m.

(C–E) Representative immunofluorescent images of YFP+ expression in back skin (C) and in lung of *Lgr5CreER/Kras*<sup>G12D</sup>/*p53*<sup>ckO</sup>/*RosaYFP* mice induced topically (D) and in lung of *Lgr5CreER/Kras*<sup>G12D</sup>/*p53*<sup>ckO</sup>/*Rosa*-tdTomato induced intra-peritoneally (E). Scale bars, 50  $\mu$ m.

(F and G) Representative immunofluorescent images of YFP+ lung metastases (F) and YFP+ LN metastases (G) arising from HF-derived tumors. Scale bars, 1 cm.

(H) Graph showing the percentage of *Lgr5CreER/Kras*<sup>G12D</sup>/*p53*<sup>ckO</sup>/*RosaYFP* mice with YFP+ lung and LN metastases (n = 70 total mice; of those, 20 mice presented lung metastases, and 34 mice had LN metastases).

(I and J) Graph showing the percentage of YFP+Epcam- TCs in metastatic (I) (mice 1–36) and non-metastatic (J) HF-derived tumors. Mice 37–54 had lung and LN metastases, mice 55–70 had only LN metastases, and mice 71 and 72 had only lung metastases (J). Each dot represents a single tumor. Red dots represent tumors above the threshold of 10% YFP+Epcam- (black line), and blue dots represent tumors below the threshold.

See also Figure S1.

Epcam- TCs found in the metastatic mice (Figures 1J and S1E–S1G) (p = 0,002 for metastatic tumors in lungs and p = 0,018 for metastatic tumors in LNs; Welch test for heterogeneity of vari-

ants). We have recently found that EMT TCs with hybrid epithelial and mesenchymal features were more metastatic than fully mesenchymal TCs upon intravenous injection (Pastushenko

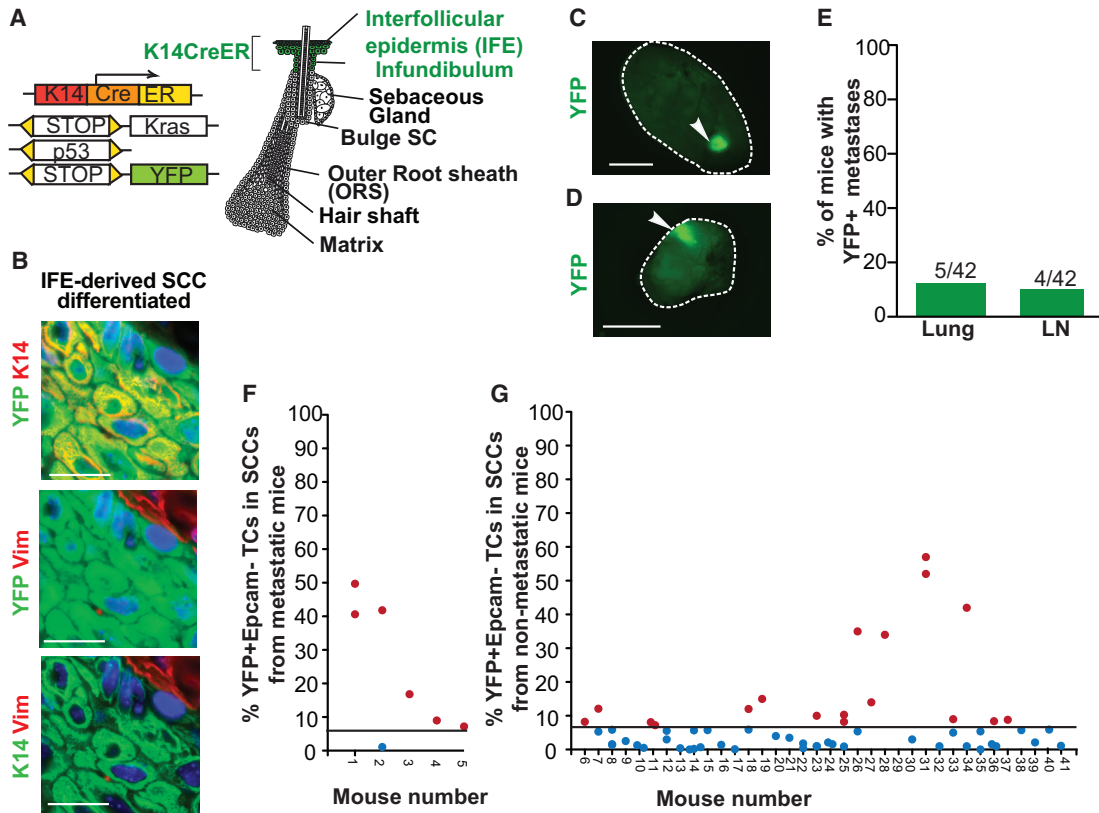


**Figure 2. IFE-Derived SCCs with a Low Rate of EMT Present a Low Incidence of Metastasis**

(A) Schematic of skin epidermis with its different lineages and the mouse model of skin SCCs with a low incidence of the EMT induced by *Kras*<sup>G12D</sup> expression and p53 deletion in IFE lineage using K14CreER.

(B) Immunofluorescence of rare metastatic SCCs in K14CreER/*Kras*<sup>G12D</sup>/p53<sup>CKO</sup>/RosaYFP mice. Scale bars, 50  $\mu$ m.

(C and D) Representative immunofluorescence of rare YFP+ lung metastases (C) and YFP+ LN metastases (D) arising from IFE-derived tumors. Scale bars, 1 cm.

(E) Graph showing the percentage of K14CreER/*Kras*<sup>G12D</sup>/p53<sup>CKO</sup>/RosaYFP mice with YFP+ lung and LN metastases (n = 42 total mice; of those, 5 mice had lung metastases, and 4 mice had LN metastases).

(F and G) Graph presenting the percentage of YFP+Epcam- TCs in metastatic (F) (mice 1–5) and non-metastatic (G) IFE-derived tumors. Mice 38–41 had lung and LN metastases; mouse 42 had only lung metastases. Each dot represents a single tumor. Red dots represent tumors above the threshold of 7% YFP+Epcam- (black line), and blue dots represent tumors below the threshold.

See also Figure S2.

et al., 2018). A FACS analysis of primary *Lgr5*-derived SCCs in mice with and without metastasis showed no statistical difference between the different subpopulations of Epcam- EMT TCs (Figure S1H), which is possibly related to the high proportion of EMT tumors without metastasis and the presence of several tumors per mice, which present metastasis. Altogether, these data show that in HF-derived primary skin SCCs that frequently undergo EMT, the occurrence of LN and lung metastases is always associated with a certain degree of EMT in the primary tumor.

### IFE-Derived SCCs with a Low Rate of EMT Present a Low Incidence of Metastasis

To assess whether primary skin SCCs rarely presenting EMT are associated with a lower frequency of metastasis compared to SCCs that frequently present EMT, we assessed the metastatic incidence and the degree of EMT in primary skin tumors arising from the expression of *Kras*<sup>G12D</sup> and p53 deletion in the IFE

lineages using K14CreER/*Kras*<sup>G12D</sup>/p53<sup>CKO</sup>/RosaYFP mice (Lapouge et al., 2012; Latil et al., 2017; White et al., 2011) (Figure 2A). Topical administration of a low dose of hydroxytamoxifen or an intraperitoneal (IP) injection of TAM to K14CreER/*Kras*<sup>G12D</sup>/p53<sup>CKO</sup>/RosaYFP mice preferentially targeted the cells of the IFE and led to an average of 2 SCCs per mouse (Figure S2A), similar to the number of tumors per mouse observed in *Lgr5* HF-derived SCCs treated with a topical application of hydroxytamoxifen (Figure S1B). As previously described (Latil et al., 2017), these mice had a very high incidence of well-differentiated SCCs (Figure 2B). The metastatic incidence observed in these mice presenting well-differentiated SCCs that rarely presented EMT was much rarer—12% (5/42) for lung and 9.5% (4/42) for LN metastases (Figures 2C–2E)—compared to the higher incidence of metastasis observed in HF-derived SCCs presenting EMT (Figure 1J). Most mice presenting lung metastases had also LN metastases (4/5), and only one mouse had exclusively lung metastases.

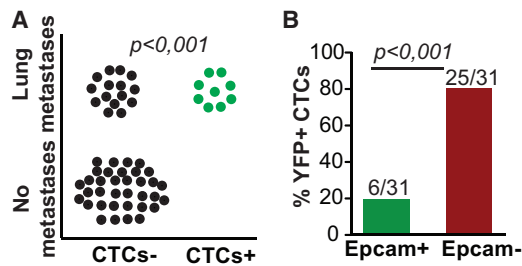


**Figure 3. Epcam-Negative CTCs Are Associated with Metastasis**  
 (A) Graph showing the presence of YFP+ CTCs and lung metastases in Lgr5CreER/Kras<sup>G12D</sup>/p53<sup>cKO</sup>/RosaYFP mice. A dot represents an individual mouse. Exact Pearson chi-square test,  $p < 0.001$ .  
 (B) Epcam expression of YFP+ CTCs from Lgr5CreER/Kras<sup>G12D</sup>/p53<sup>cKO</sup>/RosaYFP mice ( $n = 8$  mice, 31 YFP+ CTCs in total; conformity test of one proportion with  $H_0 = 0.50$ ;  $p < 0.001$ ).

As some K14CreER-derived tumors can sometimes present a low degree of EMT (Latil et al., 2017), we assessed whether the rare metastases observed in these mice present some degree of EMT by analyzing the percentage of YFP+ Epcam- TCs in the primary tumors and whether they had metastasized or not. Strikingly, all K14CreER mice that developed lung or LN metastasis had at least one primary SCC that presented some degree of EMT, with more than 7% YFP+ Epcam- TCs for mice with lung metastasis and more than 9% YFP+ Epcam- TCs for LN metastasis (Figure 2F). None of the mice presenting exclusively well-differentiated SCCs with less than 7% of YFP+ Epcam- EMT TCs developed LN or lung metastases (Figure 2G). The percentage of YFP+ Epcam- TCs for metastatic mice was higher than for non-metastatic mice ( $p < 0.001$ ). When considering the lowest percentage of Epcam values (the tumors presenting the highest EMT degree) found among the different tumors for a given mouse, the percentage of YFP+ Epcam- TCs for K14CreER mice that did not present metastasis was always higher than the percentage of YFP+ Epcam- TCs found in tumors of metastatic mice ( $p = 0.022$  for tumors with lung metastasis and  $p = 0.007$  for tumors with LN metastasis) (Figures 2F, 2G, and S2B–S2D). Altogether, these data show that mice presenting IFE-derived SCCs with no sign of EMT do not develop metastasis, and all mice presenting metastasis present some signs of EMT, further supporting the notion that at least some degree of EMT is required for spontaneous metastasis in primary skin SCC.

### Epcam-Negative CTCs Are Associated with Metastasis in Primary Skin SCC

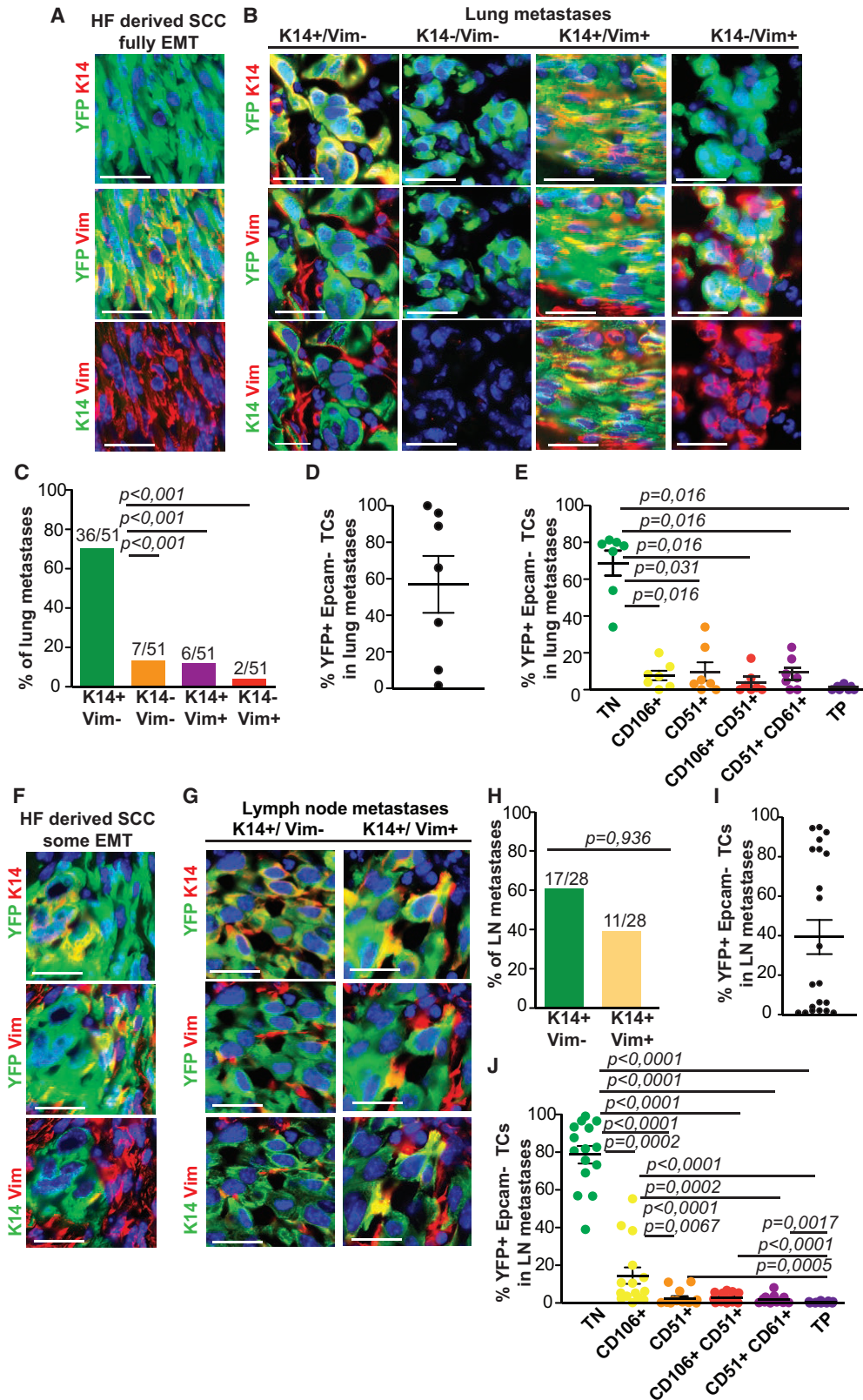
To initiate metastasis, cells must leave the primary tumor and reach the blood circulation. CTCs have been detected in the blood of patients with metastatic cancer, as well as in cancer mouse models presenting metastasis (Aceto et al., 2014; Pastushenko et al., 2018; Rhim et al., 2012; Yang et al., 2004; Yu et al., 2013). CTCs have been associated with poor prognosis in some cancers (Cristofanilli, 2006; Pantel et al., 2008). Although CTCs are usually defined as being CD45 negative, Epcam positive, and pancytokeratin positive, some recent studies indicate that CTCs present some hybrid and EMT features (Pastushenko and Blanpain, 2019; Pastushenko et al., 2018; Yu et al., 2013),

suggesting that the expression of Epcam may not be optimal to track CTCs. Our cancer mouse models with YFP-expressing TCs represent an ideal model to assess whether CTCs present some degree of EMT. We assessed the presence of CTCs in mice and whether they displayed EMT or not by quantifying the presence of CD45-/CD31- and YFP+ Epcam+ or YFP+ Epcam- cells in the peripheral blood of these mice. All mice that presented CTCs had at least one lung metastasis (Figure 3A), further supporting the notion that the presence of CTCs is associated with poor prognosis and is predictive of the presence of metastasis (Cristofanilli, 2006; Pantel et al., 2008). Interestingly, more than 80% of YFP+ CTCs were YFP+ Epcam-, showing that most CTCs presented the EMT and that Epcam-expressing CTCs represent a minor portion of total CTCs (Figure 3B). Altogether, these data show that during spontaneous lung metastasis, the cells that leave the primary tumor undergo EMT.

### Spontaneous Metastasis of Primary Tumors Is Associated with MET

While transient overexpression of the EMT TFs Twist1 and Prrx1 promotes metastasis, constitutive overexpression of the same TFs inhibits metastasis, suggesting that MET might be important for metastasis formation (Ocaña et al., 2012; Tsai et al., 2012; Yang et al., 2004). To determine whether spontaneous metastasis in primary skin SCCs is associated with MET at the metastatic site, we performed an immuno-histological analysis of epithelial and mesenchymal markers in primary SCCs as well as in lung and LN metastases from Lgr5CreER/Kras<sup>G12D</sup>/p53<sup>cKO</sup>/RosaYFP mice (Figures 4A and 4B). We found that most primary lung metastases presented the epithelial phenotype YFP+/K14+/Vim- (71% of metastases; 36/51). About 14% (7/51) of the lung metastases presented differentiated epithelial features but did not express K14 or Vimentin, 12% (6/51) of the metastases presented an EMT hybrid epithelial phenotype YFP+/K14+/Vim+, and only 4% (2/51) of the lung metastases were purely mesenchymal YFP+/K14-/Vim+ (Figure 4C). A FACS analysis of lung metastasis showed that a much lower proportion of YFP+ TCs presented EMT features, as demonstrated by the lower proportion of YFP+ Epcam- (Figure 4D) compared to the primary tumors (Figures 1I and 1J), and these Epcam- TCs were mainly composed of early hybrid EMT cells (CD106/CD51/CD61 triple negative [TN]) rather than fully mesenchymal TCs (Figure 4E), consistent with the results of the immuno-histological analysis. Likewise, the majority of LN metastases (60% of metastases; 17/28) were epithelial YFP+/K14+/Vim- (Figures 4F–4H). A greater proportion of LN metastases was composed of hybrid EMT TCs, as shown by the YFP+/K14+/Vim+ interspersed with differentiated cells (36% of metastases; 11/28) (Figures 4F–4H), and the higher proportion of Epcam- TN hybrid EMT TCs, compared to more advanced EMT states observed by the FACS analysis (Figures 4I and 4J). No metastases were composed of mesenchymal cells only (Figure 4H).

These data show that while EMT in the primary tumors and in the CTCs is important for the initial steps of metastasis, the vast majority of metastases—even those that arise from primary tumors with a high degree of EMT—are epithelial, supporting the notion that MET is important for the establishment and outgrowth of metastasis from primary skin SCCs.



(legend on next page)

### EMT Is Not Required for Metastasis Following a Transplantation of TCs

Subcutaneous transplantation of TCs is frequently used to study tumor growth and metastasis (Workman et al., 2010). We assessed whether similar mechanisms operate to mediate metastatic dissemination upon subcutaneous transplantation of TCs in immunodeficient mice, as compared to the ones we found in primary skin SCCs. To this end, we performed a subcutaneous transplantation of FACS-isolated YFP+ Epcam+ and YFP+ Epcam- TCs into immunodeficient mice and assessed the incidence of lung metastasis (no LN metastasis was observed upon tumor transplantation in NOD/SCID/Il2Rg null mice) in relation to the percentage of YFP+ Epcam+ and YFP+ Epcam- TCs in the subcutaneous tumors (Figure 5A). We used immunodeficient mice because the mice used to genetically induce SCCs (K14 and Lgr5 derived) are not inbred; therefore, TCs cannot be transplanted into syngenic mice. As previously shown, subcutaneous transplantation of YFP+ Epcam+ TCs into immunodeficient mice can give rise to well-differentiated YFP+ Epcam+ tumors or can undergo EMT and give rise to mixed YFP+ Epcam+ and YFP+ Epcam- tumors, whereas YFP+ Epcam- TCs give rise exclusively to YFP+ Epcam- tumors (Latil et al., 2017; Pastushenko et al., 2018). Surprisingly, and in sharp contrast to what we found in primary skin SCCs, we found that 58% of the transplanted tumors gave rise to metastasis irrespective of the percentage of Epcam expression, whereas tumors with less than 5% YFP+ Epcam- TCs gave rise to metastasis with the same efficiency as tumors with a high proportion of YFP+ Epcam- EMT TCs (Figure 5B). These data demonstrate that metastasis following a subcutaneous transplantation of TCs is not significantly associated with EMT.

Similar to what we found in the metastases of primary Lgr5 SCCs, the metastases that arise in secondary mesenchymal tumors following a subcutaneous transplantation of TCs were much more epithelial than their primary tumors, though a greater fraction of lung metastasis remained mesenchymal (Figures 5C and 5D). The metastases that arise from well-differentiated secondary tumors were also epithelial (Figures 5E and 5F). These data show that lung metastasis arising after a subcutaneous transplantation of TCs also frequently undergoes MET.

Mice presenting spontaneous metastasis in transplanted tumors contained CTCs resembling the primary tumors with regard to EMT. Mice with metastasis coming from tumors with little

or no EMT contained CTCs that were mainly YFP+ Epcam+, whereas mice with metastasis arising from tumors with strong EMT components presented YFP+ CTCs that were Epcam- (Figures 5G and 5H).

To assess whether the high rate of metastasis independent of EMT observed following the transplantation of Epcam+ TCs arising from Lgr5-derived SCCs was due to their HF origin, we performed a subcutaneous transplantation of YFP+ Epcam+ TCs from IFE-derived primary skin SCCs coming from K14CreER/KrasG12D/p53cKO/Rosa-YFP mice. Three out of 10 transplanted mice with Epcam+ TCs isolated from K14CreER/KrasG12D/p53cKO/Rosa-YFP mice gave rise to lung metastases (Figure S3). Among the three secondary tumors that gave rise to metastasis, one was a mixed tumor with 50% of Epcam- TCs, and the other two were well-differentiated SCCs with 12% Epcam- and 4% of Epcam- TCs (Figure S3). These data are consistent with the results obtained following the transplantation of Epcam+ TCs from Lgr5CreER/KrasG12D/p53cKO/Rosa-YFP mice and further support the notion that EMT is not absolutely essential to induce metastasis in transplanted skin SCCs independent of their cellular origin.

### DISCUSSION

In this study, we showed that spontaneous lung and LN metastases occurring in primary, genetically induced mouse SCCs were always associated with a significant fraction of EMT cells. While CTCs present in the blood of metastatic mice present EMT CTCs, most of the lung metastasis did not present residual signs of EMT, demonstrating the importance of the metastatic niche in promoting MET.

The very different metastatic incidences between the EMT-prone HF-derived SCCs and the IFE-derived well-differentiated SCCs without signs of EMT support the notion that EMT is associated with spontaneous metastasis. The precise and sensitive quantification of EMT by monitoring the percentage of YFP+ Epcam+ and YFP+ Epcam- TCs in the primary tumors demonstrated that the primary tumors of all mice presenting metastases contain a fraction of YFP+ Epcam- TCs. However, the percentage of YFP+ Epcam- TCs of the primary tumors in metastatic mice is not always a determining factor, and SCCs with as few as 7% of YFP+ Epcam- TCs can lead to metastasis. These data clearly show that careful analysis, using a very

#### Figure 4. Spontaneous Metastasis of Primary Lgr5-Derived SCCs Is Associated with MET

- (A and B) Representative immunofluorescence of K14 and Vimentin expression in a primary fully EMT tumor (A) arising from Lgr5CreER/Kras<sup>G12D</sup>/p53<sup>cKO</sup>/RosaYFP and their associated lung metastases (B). Scale bars, 50  $\mu$ m.
- (C) Graph showing the proportion of the different subtypes of YFP+ lung metastases arising from Lgr5CreER/Kras<sup>G12D</sup>/p53<sup>cKO</sup>/RosaYFP mice based on the expression of K14 and Vimentin in TCs (n = 23 mice; conformity test of one proportion with H<sub>0</sub> = 0.25; p < 0.001).
- (D) Graph showing the percentage of YFP+Epcam- TCs in lung metastases (n = 7 mice).
- (E) Graph showing subtypes of YFP+Epcam- lung metastases based on expression of CD106, CD51, and CD61. Mean and SEM are presented (n = 4 mice; Friedman test of linked samples p < 0.001; two-tailed Wilcoxon test).
- (F and G) Representative immunofluorescence of K14 and Vimentin expression in a primary tumor with a partial EMT (F) arising from Lgr5CreER/Kras<sup>G12D</sup>/p53<sup>cKO</sup>/RosaYFP and their associated LN metastases (G). Scale bars, 50  $\mu$ m.
- (H) Graph showing the proportion of the different subtypes of YFP+ LN metastases arising from Lgr5CreER/Kras<sup>G12D</sup>/p53<sup>cKO</sup>/RosaYFP mice based on the expression of K14 and Vimentin in TCs (n = 28 LNs, 28 mice; conformity test of one proportion with H<sub>0</sub> = 0.50).
- (I) Graph showing the percentage of YFP+Epcam- TCs in LN metastases (n = 13 mice, 21 LNs).
- (J) Graph showing subtypes of YFP+Epcam- LN metastases based on expression of CD106, CD51, and CD61. Mean and SEM are presented (n = 11 mice, 15 LNs; LNs with > 3% YFP+/Epcam- are represented; Friedman test of linked samples p < 0.0001; two-tailed Wilcoxon test).

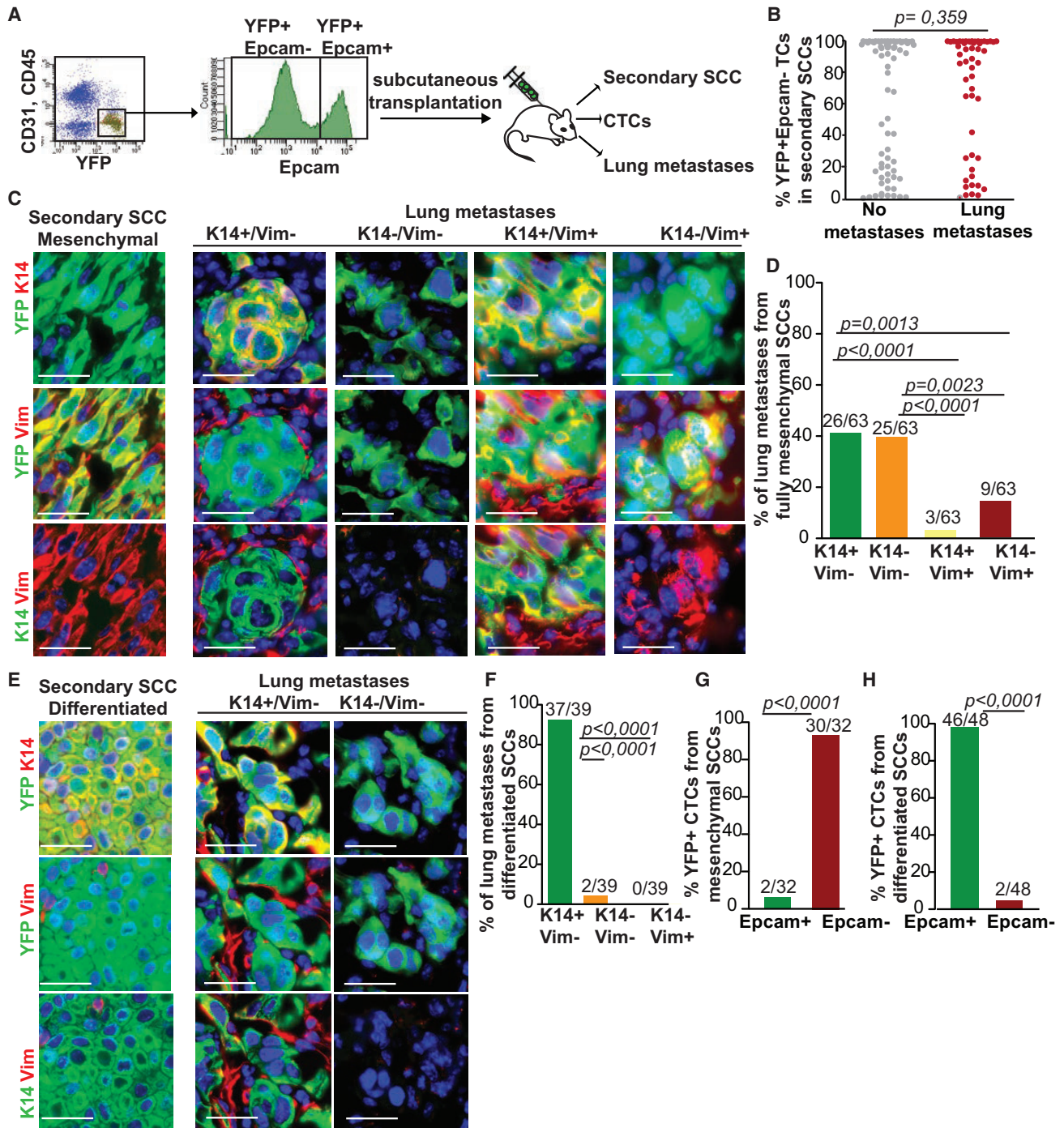


**Figure 5. EMT Is Not Required for Metastasis Following a Subcutaneous Transplantation of TCs**

(A) Experimental strategy of subcutaneously transplanted YFP+Epcam+ or YFP+Epcam- FACS-sorted TCs into NOD-SCID-Il2R $\gamma$  null mice. (B) Graph showing the percentage of YFP+Epcam- TCs in metastatic and non-metastatic tumors, showing the absence of a relationship between the proportion of Epcam-expressing TCs and the presence of lung metastases, which can occur in the absence of EMT; dots represent a single mouse with a single tumor (53 non-metastatic mice, 74 metastatic mice, two-tailed Student's t test). (C) Representative immunofluorescent images of K14 and Vimentin expression in a secondary tumor following the transplantation of Epcam- TCs from Lgr5CreER/Kras<sup>G12D</sup>/p53<sup>ckO</sup>/RosaYFP-derived SCCs into NOD-SCID-Il2R $\gamma$  null mice and their associated lung metastases. Scale bars, 50  $\mu$ m. (D) Graphs showing the proportions of the different subtypes of YFP+ lung metastases based on the co-expression of K14 and Vimentin (n = 31 mice with lung metastases arising from secondary mesenchymal SCCs; conformity test of one proportion with H<sub>0</sub> = 0.25).

(legend continued on next page)

sensitive method such as Epcam analysis by FACS in a model in which all TCs can be unambiguously identified (such as fluorescent tagging), is required to distinguish a partial EMT in the primary tumors. These data may explain the discrepancy in the interpretation of results by different groups using the same mouse models concerning the requirement of EMT for metastasis (Aiello et al., 2017; Fischer et al., 2015; Krebs et al., 2017; Rhim et al., 2012; Ye et al., 2017; Zheng et al., 2015). Importantly, not all EMT tumors give rise to metastasis, showing that while EMT is important for SCC metastasis, it represents only one of the several requirements for tumor metastasis. It has been proposed that fully mesenchymal primary tumors present lower metastatic potential (Del Pozo Martin et al., 2015). However, we found that spindle cell carcinoma, which represents fully mesenchymal tumors, can present lung and LN metastases. In Lgr5CreER-derived EMT tumors and K14CreER-derived tumors, we observed mice with lung metastasis without evidence of LN metastasis. These data support the notion that LN metastases are not an obligatory relay for lung metastasis, consistent with sequencing studies obtained in chemically-induced skin SCCs showing that LN and lung metastases often consist of different clones (Nassar et al., 2015; Westcott et al., 2015).

Detection of CTCs has been suggested to enable the stratification of patients with a high risk of developing metastasis (Effenberger et al., 2018; Krebs et al., 2014). However, the gold standard, and the only FDA-approved, method uses Epcam as a marker for CTC detection (Krebs et al., 2014). Here, we show that YFP+ CTCs were detected only in metastatic mice, suggesting that CTCs indeed correlate with the metastatic burden. However, not all mice with metastasis presented detectable CTCs, suggesting that the sensitivity of the method is not perfect. Moreover, we found that in EMT-containing tumors, most CTCs were YFP+ Epcam-, consistent with the importance of EMT order for cells to leave the primary tumors and reach the blood circulation; this shows that Epcam expression is not optimal to monitor the presence of CTCs, as many of these CTCs can lose Epcam expression (Pastushenko et al., 2018). Clearly, new markers expressed by all TCs independently of EMT will be needed to detect CTCs more accurately.

Interestingly, whereas YFP+ Epcam- TCs with partial hybrid (K14+Vim+) or complete (K14-Vim+) EMT phenotypes were present within the primary tumors that gave rise to metastasis and in CTCs from metastatic mice, most of the lung and the majority of the LN metastases were composed of epithelial TCs (K14+Vim-). In the LNs, about 40% of the metastasis also contained hybrid EMT TCs interspersed among differentiated cells, and less than 5% of the lung metastases were exclusively mesenchymal (K14-Vim+). These data clearly show that spontaneous metasta-

ses very frequently undergo MET at the metastatic site, and that the lung microenvironment promotes the epithelial phenotype more strongly than the LN microenvironment. Future studies will be needed to define the molecules that promote or restrict MET in different metastatic niches. More studies will be needed to better understand the functional consequences associated with MET during the metastatic cascade.

In sharp contrast to the metastases associated with primary skin SCCs that invariably arise from tumors containing at least a minor population that underwent EMT, metastases arising from the subcutaneous transplantation of primary TCs into immunodeficient mice can originate from purely epithelial TCs (95%–100% of YFP+ Epcam+ TCs) associated with YFP+ Epcam+ CTCs. It remains unclear why EMT is not absolutely required for metastasis under this experimental condition. Are some transplanted TCs directly pushed into the blood circulation at the time of the injection? Or do the mechanisms required for cancer cells to leave the primary tumor, circulate in the blood and establish distant metastases vary between different experimental conditions? There was a higher proportion of lung metastasis that reverted to an epithelial state in the transplanted tumors, suggesting that either the cells that undergo metastasis in transplanted tumors are less plastic than the ones arising from spontaneous metastasis, or immune cells promote MET in primary tumors from immunocompetent mice. Further studies would be required to assess the respective importance of metastasis-initiating cells and immunity in promoting EMT and MET during metastasis.

In conclusion, our study reveals the important role of EMT in promoting metastasis in different primary mouse models of SCCs and demonstrates the role of the metastatic niche in regulating MET during spontaneous metastasis. EMT and MET are not essential for lung metastasis in transplantation tumor models, demonstrating the model dependency of the EMT/MET for metastasis.

## STAR★METHODS

Detailed methods are provided in the online version of this paper and include the following:

- **KEY RESOURCES TABLE**
- **LEAD CONTACT AND MATERIALS AVAILABILITY STATEMENT**
- **EXPERIMENTAL MODEL AND SUBJECT DETAILS**
  - Mouse strains
- **METHOD DETAILS**
  - Kras<sup>LSL-G12D</sup>/p53 cKO- induced tumors
  - FACS analysis of skin tumors and metastases

(E) Representative immunofluorescent images of K14 and Vimentin expression in a secondary tumor following the transplantation of Epcam+ TCs from Lgr5CreER/Kras<sup>G12D</sup>/p53<sup>cKO</sup>/RosaYFP-derived SCCs into NOD-SCID-IL2R $\gamma$ null mice and their associated lung metastases. Scale bars, 50  $\mu$ m.

(F) Graphs showing the proportions of the different subtypes of YFP+ lung metastases based on the co-expression of K14 and Vimentin (n = 15 mice with lung metastases arising from secondary epithelial well-differentiated SCCs; conformity test of one proportion with H<sub>0</sub> = 0.25).

(G and H) Epcam expression of YFP+ CTCs in secondary mesenchymal (G) and epithelial (H) SCCs presenting lung metastasis (n = 10 mice, 32 YFP+ CTCs in total; conformity test of one proportion with H<sub>0</sub> = 0.50; p < 0.0001 for mesenchymal tumors) (n = 4 mice, 48 YFP+ CTCs in total; conformity test of one proportion with H<sub>0</sub> = 0.50; p < 0.0001 for epithelial tumors).

See also [Figure S3](#).

- Detection of CTCs
- Subcutaneous transplantation of tumor cells in immunodeficient mice
- Immunofluorescent staining
- Bioimaging
- QUANTIFICATION AND STATISTICAL ANALYSIS
- DATA AND CODE AVAILABILITY

## SUPPLEMENTAL INFORMATION

Supplemental Information can be found online at <https://doi.org/10.1016/j.celrep.2019.09.081>.

## ACKNOWLEDGMENTS

We thank the ULB animal house facility. We thank Andrea Karambelas for proofreading and Sebastien Delcambre for the follow-up of the grafted mice. T.R. was supported by the FNRS/FRIA and Rose and Jean Hogue Foundation. C.B. is supported by WELBIO, FNRS, Fondation Contre le Cancer, ULB Foundation, European Research Council, Worldwide Cancer Research, and the Foundation Baillet Latour.

## AUTHOR CONTRIBUTIONS

T.R. and C.B. designed the experiments and performed data analysis. T.R. performed most of the biological experiments, FACS analysis, and histological characterization. A.N. performed some biological experiments, FACS analysis, and histological characterization. M.K.S. provided assistance with some experiments. I.P. performed part of the histological analysis. M.L. and P.A.S. performed the experimental setup. C.D. performed FACS sorting. V.M. and S.L. performed PCRs for mouse genotyping. V.d.M. performed the statistical analysis. All authors read and approved the final manuscript. Correspondence and requests for materials should be addressed to C.B.

## DECLARATION OF INTERESTS

The authors declare no competing interests.

Received: June 9, 2019

Revised: August 23, 2019

Accepted: September 26, 2019

Published: November 5, 2019

## REFERENCES

- Aceto, N., Bardia, A., Miyamoto, D.T., Donaldson, M.C., Wittner, B.S., Spencer, J.A., Yu, M., Pely, A., Engstrom, A., Zhu, H., et al. (2014). Circulating tumor cell clusters are oligoclonal precursors of breast cancer metastasis. *Cell* 158, 1110–1122.
- Aiello, N.M., Brabletz, T., Kang, Y., Nieto, M.A., Weinberg, R.A., and Stanger, B.Z. (2017). Upholding a role for EMT in pancreatic cancer metastasis. *Nature* 547, E7–E8.
- Barker, N., van Es, J.H., Kuipers, J., Kujala, P., van den Born, M., Cozijnsen, M., Haegebarth, A., Korving, J., Begthel, H., Peters, P.J., and Clevers, H. (2007). Identification of stem cells in small intestine and colon by marker gene *Lgr5*. *Nature* 449, 1003–1007.
- Celià-Terrassa, T., Meca-Cortés, O., Mateo, F., Martínez de Paz, A., Rubio, N., Arnal-Estapé, A., Eli, B.J., Bermudo, R., Díaz, A., Guerra-Rebollo, M., et al. (2012). Epithelial-mesenchymal transition can suppress major attributes of human epithelial tumor-initiating cells. *J. Clin. Invest.* 122, 1849–1868.
- Chaffer, C.L., Thompson, E.W., and Williams, E.D. (2007). Mesenchymal to epithelial transition in development and disease. *Cells Tissues Organs (Print)* 185, 7–19.
- Cristofanilli, M. (2006). Circulating tumor cells, disease progression, and survival in metastatic breast cancer. *Semin. Oncol.* 33, S9–S14.
- Del Pozo Martin, Y., Park, D., Ramachandran, A., Ombrato, L., Calvo, F., Chakravarty, P., Spencer-Dene, B., Derzi, S., Hill, C.S., Sahai, E., and Malanchi, I. (2015). Mesenchymal Cancer Cell-Stroma Crosstalk Promotes Niche Activation, Epithelial Reversion, and Metastatic Colonization. *Cell Rep.* 13, 2456–2469.
- Diepenbruck, M., and Christofori, G. (2016). Epithelial-mesenchymal transition (EMT) and metastasis: yes, no, maybe? *Curr. Opin. Cell Biol.* 43, 7–13.
- Effenberger, K.E., Schroeder, C., Hanssen, A., Wolter, S., Eulenburg, C., Tachezy, M., Gebauer, F., Izbicki, J.R., Pantel, K., and Bockhorn, M. (2018). Improved Risk Stratification by Circulating Tumor Cell Counts in Pancreatic Cancer. *Clin. Cancer Res.* 24, 2844–2850.
- Fischer, K.R., Durrans, A., Lee, S., Sheng, J., Li, F., Wong, S.T., Choi, H., El Rayes, T., Ryu, S., Troeger, J., et al. (2015). Epithelial-to-mesenchymal transition is not required for lung metastasis but contributes to chemoresistance. *Nature* 527, 472–476.
- Gunasinghe, N.P., Wells, A., Thompson, E.W., and Hugo, H.J. (2012). Mesenchymal-epithelial transition (MET) as a mechanism for metastatic colonisation in breast cancer. *Cancer Metastasis Rev.* 31, 469–478.
- Jonkers, J., Meuwissen, R., van der Gulden, H., Peterse, H., van der Valk, M., and Berns, A. (2001). Synergistic tumor suppressor activity of BRCA2 and p53 in a conditional mouse model for breast cancer. *Nat. Genet.* 29, 418–425.
- Krebs, M.G., Metcalf, R.L., Carter, L., Brady, G., Blackhall, F.H., and Dive, C. (2014). Molecular analysis of circulating tumour cells-biology and biomarkers. *Nat. Rev. Clin. Oncol.* 11, 129–144.
- Krebs, A.M., Mitschke, J., Laserra Losada, M., Schmalhofer, O., Boerries, M., Busch, H., Boettcher, M., Mougiakakos, D., Reichardt, W., Bronsert, P., et al. (2017). The EMT-activator Zeb1 is a key factor for cell plasticity and promotes metastasis in pancreatic cancer. *Nat. Cell Biol.* 19, 518–529.
- Lambert, A.W., Pattabiraman, D.R., and Weinberg, R.A. (2017). Emerging Biological Principles of Metastasis. *Cell* 168, 670–691.
- Lapouge, G., Beck, B., Nassar, D., Dubois, C., Dekoninck, S., and Blanpain, C. (2012). Skin squamous cell carcinoma propagating cells increase with tumour progression and invasiveness. *EMBO J.* 31, 4563–4575.
- Latil, M., Nassar, D., Beck, B., Boumahdi, S., Wang, L., Brisebarre, A., Dubois, C., Nkusi, E., Lenglez, S., Chęcinska, A., et al. (2017). Cell-Type-Specific Chromatin States Differentiate Prime Squamous Cell Carcinoma Tumor-Initiating Cells for Epithelial to Mesenchymal Transition. *Cell Stem Cell* 20, 191–204.e195.
- Lee, J.H., Tammela, T., Hofree, M., Choi, J., Marjanovic, N.D., Han, S., Canner, D., Wu, K., Paschini, M., Bhang, D.H., et al. (2017). Anatomically and Functionally Distinct Lung Mesenchymal Populations Marked by *Lgr5* and *Lgr6*. *Cell* 170, 1149–1163.e1112.
- Massagué, J., and Obenauf, A.C. (2016). Metastatic colonization by circulating tumour cells. *Nature* 529, 298–306.
- Mehlen, P., and Puisieux, A. (2006). Metastasis: a question of life or death. *Nat. Rev. Cancer* 6, 449–458.
- Mittal, V. (2018). Epithelial Mesenchymal Transition in Tumor Metastasis. *Annu. Rev. Pathol.* 13, 395–412.
- Nassar, D., Latil, M., Boeckx, B., Lambrechts, D., and Blanpain, C. (2015). Genomic landscape of carcinogen-induced and genetically induced mouse skin squamous cell carcinoma. *Nat. Med.* 21, 946–954.
- Nieto, M.A., Huang, R.Y., Jackson, R.A., and Thiery, J.P. (2016). EMT: 2016. *Cell* 166, 21–45.
- Ocaña, O.H., Córcoles, R., Fabra, A., Moreno-Bueno, G., Acloque, H., Vega, S., Barrallo-Gimeno, A., Cano, A., and Nieto, M.A. (2012). Metastatic colonization requires the repression of the epithelial-mesenchymal transition inducer *Prrx1*. *Cancer Cell* 22, 709–724.
- Olmeda, D., Moreno-Bueno, G., Flores, J.M., Fabra, A., Portillo, F., and Cano, A. (2007). SNAI1 is required for tumor growth and lymph node metastasis of human breast carcinoma MDA-MB-231 cells. *Cancer Res.* 67, 11721–11731.

- Pantel, K., Brakenhoff, R.H., and Brandt, B. (2008). Detection, clinical relevance and specific biological properties of disseminating tumour cells. *Nat. Rev. Cancer* 8, 329–340.
- Pastushenko, I., and Blanpain, C. (2019). EMT Transition States during Tumor Progression and Metastasis. *Trends Cell Biol.* 29, 212–226.
- Pastushenko, I., Brisebarre, A., Sifrim, A., Fioramonti, M., Revenco, T., Boumahdi, S., Van Keymeulen, A., Brown, D., Moers, V., Lemaire, S., et al. (2018). Identification of the tumour transition states occurring during EMT. *Nature* 556, 463–468.
- Rhim, A.D., Mirek, E.T., Aiello, N.M., Maitra, A., Bailey, J.M., McAllister, F., Reichert, M., Beatty, G.L., Rustgi, A.K., Vonderheide, R.H., et al. (2012). EMT and dissemination precede pancreatic tumor formation. *Cell* 148, 349–361.
- Schmidt, J.M., Panzilius, E., Bartsch, H.S., Irmeler, M., Beckers, J., Kari, V., Linnemann, J.R., Dragoi, D., Hirschi, B., Kloos, U.J., et al. (2015). Stem-cell-like properties and epithelial plasticity arise as stable traits after transient Twist1 activation. *Cell Rep.* 10, 131–139.
- Srinivas, S., Watanabe, T., Lin, C.S., William, C.M., Tanabe, Y., Jessell, T.M., and Costantini, F. (2001). Cre reporter strains produced by targeted insertion of EYFP and ECFP into the ROSA26 locus. *BMC Dev. Biol.* 1, 4.
- Stankic, M., Pavlovic, S., Chin, Y., Brogi, E., Padua, D., Norton, L., Massagué, J., and Benezra, R. (2013). TGF- $\beta$ -Id1 signaling opposes Twist1 and promotes metastatic colonization via a mesenchymal-to-epithelial transition. *Cell Rep.* 5, 1228–1242.
- Takano, S., Reichert, M., Bakir, B., Das, K.K., Nishida, T., Miyazaki, M., Heeg, S., Collins, M.A., Marchand, B., Hicks, P.D., et al. (2016). Prrx1 isoform switching regulates pancreatic cancer invasion and metastatic colonization. *Genes Dev.* 30, 233–247.
- Tsai, J.H., Donaher, J.L., Murphy, D.A., Chau, S., and Yang, J. (2012). Spatio-temporal regulation of epithelial-mesenchymal transition is essential for squamous cell carcinoma metastasis. *Cancer Cell* 22, 725–736.
- Tuveson, D.A., Shaw, A.T., Willis, N.A., Silver, D.P., Jackson, E.L., Chang, S., Mercer, K.L., Grochow, R., Hock, H., Crowley, D., et al. (2004). Endogenous oncogenic K-ras(G12D) stimulates proliferation and widespread neoplastic and developmental defects. *Cancer Cell* 5, 375–387.
- Vasioukhin, V., Degenstein, L., Wise, B., and Fuchs, E. (1999). The magical touch: genome targeting in epidermal stem cells induced by tamoxifen application to mouse skin. *Proc. Natl. Acad. Sci. USA* 96, 8551–8556.
- Westcott, P.M., Halliwill, K.D., To, M.D., Rashid, M., Rust, A.G., Keane, T.M., Delrosario, R., Jen, K.Y., Gurley, K.E., Kemp, C.J., et al. (2015). The mutational landscapes of genetic and chemical models of Kras-driven lung cancer. *Nature* 517, 489–492.
- White, A.C., Tran, K., Khuu, J., Dang, C., Cui, Y., Binder, S.W., and Lowry, W.E. (2011). Defining the origins of Ras/p53-mediated squamous cell carcinoma. *Proc. Natl. Acad. Sci. USA* 108, 7425–7430.
- Workman, P., Aboagye, E.O., Balkwill, F., Balmain, A., Bruder, G., Chaplin, D.J., Double, J.A., Everitt, J., Farningham, D.A., Glennie, M.J., et al.; Committee of the National Cancer Research Institute (2010). Guidelines for the welfare and use of animals in cancer research. *Br. J. Cancer* 102, 1555–1577.
- Xu, Y., Lee, D.K., Feng, Z., Xu, Y., Bu, W., Li, Y., Liao, L., and Xu, J. (2017). Breast tumor cell-specific knockout of *Twist1* inhibits cancer cell plasticity, dissemination, and lung metastasis in mice. *Proc. Natl. Acad. Sci. USA* 114, 11494–11499.
- Yang, J., Mani, S.A., Donaher, J.L., Ramaswamy, S., Itzykson, R.A., Come, C., Savagner, P., Gitelman, I., Richardson, A., and Weinberg, R.A. (2004). Twist, a master regulator of morphogenesis, plays an essential role in tumor metastasis. *Cell* 117, 927–939.
- Yao, D., Dai, C., and Peng, S. (2011). Mechanism of the mesenchymal-epithelial transition and its relationship with metastatic tumor formation. *Mol. Cancer Res.* 9, 1608–1620.
- Ye, X., Brabletz, T., Kang, Y., Longmore, G.D., Nieto, M.A., Stanger, B.Z., Yang, J., and Weinberg, R.A. (2017). Upholding a role for EMT in breast cancer metastasis. *Nature* 547, E1–E3.
- Yu, M., Bardia, A., Wittner, B.S., Stott, S.L., Smas, M.E., Ting, D.T., Isakoff, S.J., Ciciliano, J.C., Wells, M.N., Shah, A.M., et al. (2013). Circulating breast tumor cells exhibit dynamic changes in epithelial and mesenchymal composition. *Science* 339, 580–584.
- Zepp, J.A., Zacharias, W.J., Frank, D.B., Cavanaugh, C.A., Zhou, S., Morley, M.P., and Morrissey, E.E. (2017). Distinct Mesenchymal Lineages and Niches Promote Epithelial Self-Renewal and Myofibrogenesis in the Lung. *Cell* 170, 1134–1148.e1110.
- Zheng, X., Carstens, J.L., Kim, J., Scheible, M., Kaye, J., Sugimoto, H., Wu, C.C., LeBleu, V.S., and Kalluri, R. (2015). Epithelial-to-mesenchymal transition is dispensable for metastasis but induces chemoresistance in pancreatic cancer. *Nature* 527, 525–530.

## STAR★METHODS

### KEY RESOURCES TABLE

REAGENT or RESOURCE	SOURCE	IDENTIFIER
<b>Antibodies</b>		
Goat anti-GFP	Abcam	Cat#ab6673
Chicken anti-K14 (polyclonal)	Thermo Fisher Scientific	Cat#MA5-11599
Rabbit anti-Epcam	Abcam	Cat#ab6673
Rabbit anti-Vimentin	Abcam	Cat#ab92547
Chicken anti-GFP	Abcam	Cat#ab13970
anti-rabbit conjugated to rhodamine Red-X	Jackson ImmunoResearch	Cat#711-295-152
anti-chicken conjugated to rhodamine Red-X	Jackson ImmunoResearch	Cat#703-295-155
anti-rabbit conjugated to rhodamine Cy5	Jackson ImmunoResearch	Cat#711-605-152
anti-goat conjugated to Alexa Fluor-A488	Invitrogen ThermoFisher	Cat#A11055
anti-chicken conjugated to Alexa Fluor-A488	Invitrogen ThermoFisher	Cat#A11039
Rat BV711- conjugated anti-Epcam (clone G8.8)	BD Bioscience	Cat#563134
Rat PerCPCy5.5-conjugated anti-CD45(clone 30-F11)	BD Bioscience	Cat#550994
Rat PerCPCy5.5-conjugated anti-CD31 (clone MEC 13.3)	BD Bioscience	Cat#562861
streptavidin-BV786	BD Bioscience	Cat#563858
PE-conjugated anti-CD51 (rat clone RMV-7)	Biolegend	Cat#104106
BV421-conjugated anti-CD61 (armenian hamster, clone 2C9.G2)	BD Bioscience	Cat#553345
CD106 (rat, clone 429 (MVCAM.A)	BD Bioscience	Cat#553331
<b>Chemicals, Peptides, and Recombinant Proteins</b>		
4-Hydroxytamoxifen	Sigma	Cat#H6278-50MG
Tamoxifen	Sigma	Cat#T5648-5G
Matrigel	Sigma	Cat#E1270
Collagenase type 1	Sigma	Cat#234153
HBSS without Ca	Invitrogen	Cat#14175095
EDTA	Ambion	P/N: AM9260G, L/N: 1509002)
<b>Experimental Models: Organisms/Strains</b>		
NOD/SCID/IL2R $\gamma$ null mice	Charles River	N/A
Rosa26-YFP mice	Jackson Laboratories	<a href="#">Srinivas et al., 2001</a>
Lgr5CreER mice	Jackson Laboratories	<a href="#">Barker et al., 2007</a>
K14CreER mice	Jackson Laboratories	<a href="#">Vasioukhin et al., 1999</a>
KRas <sup>LSL-G12D</sup> mice	Jackson Laboratories	<a href="#">Tuveson et al., 2004</a>
p53cKO mice	Jackson Laboratories	<a href="#">Jonkers et al., 2001</a>
<b>Software and Algorithms</b>		
Adobe illustrator CC (version 17.1.0)	Adobe	<a href="https://www.adobe.com/be_fr/downloads.html">https://www.adobe.com/be_fr/downloads.html</a>
Photoshop CS3	Adobe	<a href="https://www.adobe.com/be_fr/downloads.html">https://www.adobe.com/be_fr/downloads.html</a>
SPSS (version 25.0)	IBM Corp, Armonk, NY, USA	N/A
MedCalc (version 14.12.0)	MedCalc Software bvba, Ostend, Belgium;2014	<a href="http://www.medcalc.org">http://www.medcalc.org</a>
Microsoft Office 365 Excel	Microsoft	RRID SCR_016137
Graph Pad Prism (version 5.0a)	GraphPad	RRID SCR_002798

## LEAD CONTACT AND MATERIALS AVAILABILITY STATEMENT

Further information and requests for resources and reagents should be directed to and will be fulfilled by the Lead Contact, Cédric Blanpain ([Cedric.blanpain@ulb.ac.be](mailto:Cedric.blanpain@ulb.ac.be)). This study did not generate new unique reagents.

## EXPERIMENTAL MODEL AND SUBJECT DETAILS

Mouse colonies were maintained in a certified animal facility in accordance with the European guidelines. All the experiments were approved by the corresponding ethical committee (Commission d'Ethique et du Bien Etre Animal CEBEA, Faculty of Medicine, Université Libre de Bruxelles). CEBEA follows the European Convention for the Protection of Vertebrate Animals used for Experimental and other Scientific Purposes (ETS No.123). Mice were checked every day and were euthanized when the tumor reached the end-point size (1 cm in diameter or 1 cm<sup>3</sup> in volume) or if the tumor was ulcerated (independent of its size), if the mouse lost >20% of its initial weight or showed any other sign of distress (based on general health status and spontaneous activity). None of the experiments performed in this study surpassed the size limit of the tumors fixed in the Ethical protocol. All the experiments complied strictly with the protocols approved by Ethical Committee.

### Mouse strains

Rosa26-YFP mice (Srinivas et al., 2001), Lgr5CreER mice (Barker et al., 2007), K14CreER mice (Vasioukhin et al., 1999), KRas<sup>LSL-G12D</sup> (Tuveson et al., 2004) mice and p53 floxed (Jonkers et al., 2001) mice were imported from the NCI mouse repository and Jackson Laboratories. All mice used in this study were composed of males and females with mixed genetic background. No randomization and no blinding were performed in this study.

## METHOD DETAILS

### Kras<sup>LSL-G12D</sup>/p53 cKO- induced tumors

Lgr5CreER/Kras<sup>G12D</sup>/p53<sup>cKO</sup>/RosaYFP mice were induced with tamoxifen by one topical application on shaved back skin between scapulae (10 mg/ml; 100  $\mu$ L per mouse). K14CreER/Kras<sup>G12D</sup>/p53<sup>cKO</sup>/RosaYFP were induced with tamoxifen by intraperitoneal injections (2,5 mg 1x) or by one topical application on shaved back skin between scapulae (10 mg/ml; 100  $\mu$ L per mouse). All mice were 28-35 days old at the moment of induction. Tumor appearance was monitored by daily observation. Mice were sacrificed when the tumors reached the size limit of 1 cm<sup>3</sup> in diameter or when mice presented signs of distress. Skin tumors were measured by precision caliper, enabling the identification of 0,1 mm change in size. Tumor volume was calculated using the formula  $V = \pi(d^2D)/6$ , where d is the minor tumor axis and D is the perpendicular major tumor axis. At the moment of sacrifice skin tumors, blood, lung, and lymph nodes were collected.

### FACS analysis of skin tumors and metastases

Skin tumors from Lgr5CreER/Kras<sup>G12D</sup>/p53<sup>cKO</sup>/RYFP, K14CreER/Kras<sup>G12D</sup>/p53<sup>cKO</sup>/RosaYFP and transplanted NOD/SCID/Il2R $\gamma$  null mice, and metastases from lung and lymph nodes of Lgr5CreER/Kras<sup>G12D</sup>/p53<sup>cKO</sup>/RosaYFP mice were dissected, minced, and digested in Collagenase type 1 (Sigma) 3,5 mg/ml diluted in HBSS without Ca (Invitrogen) for 1 h at 37°C on a rocking plate protected from light. Collagenase activity was blocked by the addition of EDTA (0.5 M, pH 8, Ambion P/N: AM9260G, L/N: 1509002) and then the cells were rinsed in PBS supplemented with 10% FBS and the cell suspensions were filtered through a 70- $\mu$ m cell strainer (BD Bioscience). Brilliant violet stain buffer (BD Bioscience) was added (50  $\mu$ L per sample) and the cells were incubated with primary antibodies for 30 min at 4°C protected from light. The following primary antibodies were used: BV711- conjugated anti-Epcam (rat clone G8.8, BD Bioscience Cat#563134, dilution 1:100), PerCPCy5.5-conjugated anti-CD45 (rat, clone 30-F11, BD Bioscience Cat#550994, dilution 1:100), PerCPCy5.5-conjugated anti-CD31 (rat, clone MEC 13.3, BD Bioscience Cat#562861, dilution 1:100), PE-conjugated anti-CD51 (rat clone RMV-7, Biolegend Cat#104106, dilution 1:50), BV421-conjugated anti-CD61 (armenian hamster, clone 2C9.G2, BD Cat#553345, dilution 1:50), biotinconjugated anti-CD106 (rat, clone 429 (MVCAM.A), BD Cat#553331, dilution 1:50).

Cells were washed with PBS supplemented with 2% FBS and incubated 30 min protected on ice with secondary antibody streptavidin-BV786 (BD Bioscience Cat#563858, dilution 1:400). Living single TCs were selected by forward and side scatter, doublet discrimination and 7AAD dye exclusion. FACS analyses were performed with Fortessa and FACS DiVa software (BD Biosciences). Cell sorting was performed with FACS Aria cell sorter (BD Biosciences).

### Detection of CTCs

1 mL blood was extracted by cardiac cord disrupter with 100  $\mu$ L EDTA (0.5 M, pH 8, Ambion P/N: AM9260G, L/N: 1509002). Red blood cells were lysed with 0.2% NaCl (VWR chemicals) and brought to isotonic condition with 3.8% NaCl, 0.2% sucrose (MERCK KGaA). The blood was incubated with collagenase type 1 (Sigma) at 37°C for 30 min protected from light on rocking plate to dissociate CTC clusters. FACS staining and analysis were performed as described for tumors.

### Subcutaneous transplantation of tumor cells in immunodeficient mice

NOD/SCID/Il2R $\gamma$  null mice were purchased from Charles River. All mice used in this study were composed of males and females, of the same age. Tumors were dissected, minced, and digested as described above for the FACS analysis. Tumor cells were selected by YFP expression and the exclusion of CD45 and CD31 from SCCs of Lgr5CreER/Kras<sup>G12D</sup>/p53<sup>ckO</sup>/RosaYFP and K14CreER/Kras<sup>G12D</sup>/p53<sup>ckO</sup>/RosaYFP mice. FACS-sorted YFP+/Epcam+/CD31-/CD45- TCs and YFP+/Epcam-/CD31-/CD45- TCs (100, 500 and 5.000 TCs) were resuspended in 50  $\mu$ l matrigel (E1270, 970 mg/ml; Sigma) and subcutaneously injected into NOD/SCID/Il2R $\gamma$  null mice (1 injection per mouse). Mice were sacrificed when the tumor reached size limit of 1 cm<sup>3</sup>. Secondary skin tumors, blood, and lung were collected.

### Immunofluorescent staining

At the moment of mouse sacrifice tumors, lung and LNs were prefixed in 4% paraformaldehyde for 2h at room temperature, followed by sucrose 30% over-night, subsequently washed with PBS and embedded in OCT.

Non-specific antibody binding was blocked with 5% horse serum, 1% BSA, 0.1% triton x-100 for 1 h at room temperature. Primary antibodies were incubated over night at 4°C. Secondary antibodies were incubated for 1h at room temperature. Mounting of slides was performed with Glycergel (Dako) supplemented with 2, 5% 1, 4- Diazobicyclo (2, 2, 2) octane (DABCO; Sigma-Aldrich). The phenotype and the number of metastases were quantified on 10 serial cryosections per lung (separated by 100  $\mu$ m) based on YFP expression.

The following primary antibodies were used: anti-GFP (goat polyclonal, Abcam Cat#ab6673, dilution 1:500), anti-K14 (chicken polyclonal, Thermo Fisher Scientific Cat#MA5-11599, dilution 1:1500), anti-Vimentin (rabbit, clone ERP3776 Abcam Cat#ab92547, dilution 1:500), anti-GFP chk (Abcam, dilution 1:4000), anti-Epcam rb (Abcam, dilution 1:200). The following secondary antibodies were used (all at dilution 1:400): anti-rabbit, anti-rat, anti-goat, anti-chicken conjugated to rhodamine Red-X (Jackson ImmunoResearch), Cy5 (Jackson ImmunoResearch) or Alexa Fluor-A488 (Molecular Probes).

### Bioimaging

Image acquisition was performed on Zeiss Axio Imager M1 (Thornwood) fluorescent microscope with a Zeiss AxioCam MR3 cameras, using Axiovision release 4.6 software. Single cell pictures were acquired with the same microscope supplied with 100x objective (alfa-Plan-Fluor 1.45 numerical aperture oil-immersion objective). The picture sizes were adjusted using Photoshop CS3 (Adobe) software.

## QUANTIFICATION AND STATISTICAL ANALYSIS

Continuous variables are given as means and standard error of the mean (SEM) and qualitative variables as percentages.

Differences in continuous variables were compared between two groups using parametric tests (classical t test or Welch test in case of heterogeneity) in case of large enough sample sizes or Mann Whitney tests otherwise. Comparisons among independent groups in case of qualitative variables were performed using exact Pearson chi-square tests. Conformity tests were performed for testing the null hypothesis of equal proportions ( $H_0 = 0.50$  in case of two groups and  $H_0 = 0.25$  in case of four groups). For repeated data, Friedman tests were performed, followed by two by two Wilcoxon tests in case of statistical significance.

Statistical significance was considered when  $p$  was  $< 0.05$ . All statistical tests were performed using IBM-SPSS (version 25.0) software (IBM Corp, Armonk, NY, USA) and MedCalc (version 14.12.0) Statistical Software (MedCalc Software bvba, Ostend, Belgium; <http://www.medcalc.org>; 2014).

All statistical analyses were based on biological replicates (n indicated in the text, figures or figure legends). No technical replicates were used to calculate statistics.

## DATA AND CODE AVAILABILITY

This study did not generate any unique datasets or code.